Non-Poissonian Exciton Populations in Semiconductor Nanocrystals via Carrier Multiplication

Richard D. Schaller and Victor I. Klimov*

Chemistry Division, C-PCS, Los Alamos National Laboratory, Los Alamos, New Mexico 87545, USA

(Received 19 October 2005; published 7 March 2006)

We analyze distributions of exciton populations in PbSe nanocrystal (NC) ensembles as a function of excitation wavelength. For photon energies that result in carrier multiplication, these distributions are non-Poissonian and are characterized by two dominant exciton multiplicities that are determined by the ratio of photon energy to NC energy gap. For certain photon energies, we produce photoexcited NC ensembles with a nearly pure single multiplicity that can be tuned from 1 to 7. This result can find applications ranging from lasing and nonlinear optics to photovoltaics and photocatalysis.

DOI: 10.1103/PhysRevLett.96.097402 PACS numbers: 78.67.Bf, 71.35.−y, 73.21.La, 78.47.+p

Nanocrystal (NC) quantum dots are nanoscale semiconductor particles in which carrier motion is confined in all three dimensions [1,2]. This 3D confinement leads to a discrete structure of energy states that can be controlled by NC size [3]. Another result of strong confinement in NCs is greatly enhanced exciton-exciton interactions that lead, e.g., to large biexciton binding energies [4,5] and high-efficiency nonradiative recombination of multiexcitons via Auger recombination [6,7]. Normally, multiexcitons in NCs are generated via sequential absorption of multiple photons using high-intensity, pulsed laser excitation. In this case, the exciton multiplicity differs across the NC ensemble and its distribution is described by Poissonian statistics [8]. The ability to produce multiexcitons of a given multiplicity uniformly across a NC ensemble could significantly benefit both fundamental studies of exciton-exciton interactions in strongly confined systems as well as a number of NC applications that rely on multiexcitons such as optical amplification and lasing [9].

In this Letter, we demonstrate that by using the newly discovered phenomenon of high-efficiency carrier multiplication (CM) [10–12], we can produce multiexciton states of a controlled multiplicity in a NC ensemble. In the CM process, multiexcitons are generated from single photons and their multiplicity is determined not by the pump intensity (as in the no-CM case) but by the pump-photon energy. This phenomenon can be explained in terms of direct, instantaneous generation of multiexcitons via strong confinement-enhanced coupling to *virtual* single-exciton states [12]. Using this process, we demonstrate photoexcited ensembles of PbSe NCs with nearly pure single multiplicity that can be tuned from 1 to 7. The process studied in this work allows for production of high-order multiexcitons using low intensity and even incoherent cw radiation sources, i.e., the conditions under which multiexciton generation in NCs by the traditional process of absorption of multiple photons is not efficient.

To detect CM and quantify the exciton multiplicity produced by this effect, we monitor NC carrier population dynamics using femtosecond transient absorption (TA). In this experiment, colloidal PbSe NCs fabricated according to Ref. [13] are excited with sub-100 fs spectrally tunable pulses from an optical parametric amplifier that is pumped by a 1 kHz, amplified Ti:sapphire laser. Pump-induced absorption changes are probed at the position of the lowest-energy $1S$ absorption peak with a second tunable, time-delayed sub-100 fs pulse. Single- and multiexciton species are distinguished based on a significant difference in their relaxation dynamics (sub-μs [14,15] vs ps [10] time scales for excitons and multiexcitons, respectively). As a result of this difference, the generation of multiexcitons from a single absorbed photon can be detected via a fast Auger-decay component in TA dynamics, while the magnitude of this component can be used to quantify the CM efficiency [10]. Specifically, the ratio of the amplitude of the TA trace immediately after excitation to the height of the long-lived, single-exciton background provides a direct measure of average exciton multiplicity, $\langle N_x \rangle$, which is defined as the average number of excitons per NC within a subensemble of photoexcited NCs [10,12].

When multiexcitons are generated by high-intensity pump pulses via the traditional process of absorption of multiple photons (no CM), NC exciton populations exhibit a Poissonian distribution [8]. In this case, the average number of excitons per NC, $\langle N_0 \rangle$, is simply proportional to the per-pulse pump fluence, j_p ($\langle N_0 \rangle = j_p \sigma_a$; σ_a is the NC absorption cross section [8]); the pump fluence also determines the average exciton multiplicity in photoexcited NCs: $\langle N_x \rangle = \langle N_0 \rangle (1 - e^{-\langle N_0 \rangle})^{-1}$. An interesting feature of the photoexcited system produced by CM is that it is *non-Poissonian*. At low pump intensities ($j_p \sigma_a \ll 1$), for which the probability of generating multiexcitons via absorption of multiple photons is negligibly small, $\langle N_x \rangle$ is determined not by the pump fluence but by the pump-photon energy, $\hbar\omega$. Furthermore, in this case, the maximum possible exciton multiplicity is limited by $f = \lfloor \hbar\omega / E_g \rfloor$ (E_g is the NC energy gap, "$\lfloor X \rfloor$" and "$\lceil X \rceil$" indicate the rounded-down and rounded-up integer values of X, respectively) because of the energy conservation requirement.

The difference in the distribution of carrier populations with and without CM is evident from pump-intensity-

dependent TA dynamics measured for PbSe NCs with photon energies below and above the CM threshold ($\hbar\omega_{CM} = 2.85E_g$) [Figs. 1(a) and 1(b)]. In both cases, the fast TA component originates from the Auger decay of multiexcitons. However, the pump dependence of this component is quite different in the CM and no-CM cases. Without CM, the fast-component amplitude tends to zero with decreasing pump level, which corresponds to $\langle N_x\rangle \to 1$, as expected for the Poissonian distribution [compare open squares (experiment) and line (calculated Poissonian probabilities) in Fig. 1(c)]. In the CM case, the fast component shows non-Poissonian behavior [solid circles in Fig. 1(c)], and specifically, it persists in the limit of zero pump intensity, which indicates that multiexcitons are produced from single photons, i.e., via a *pump-intensity-independent* process.

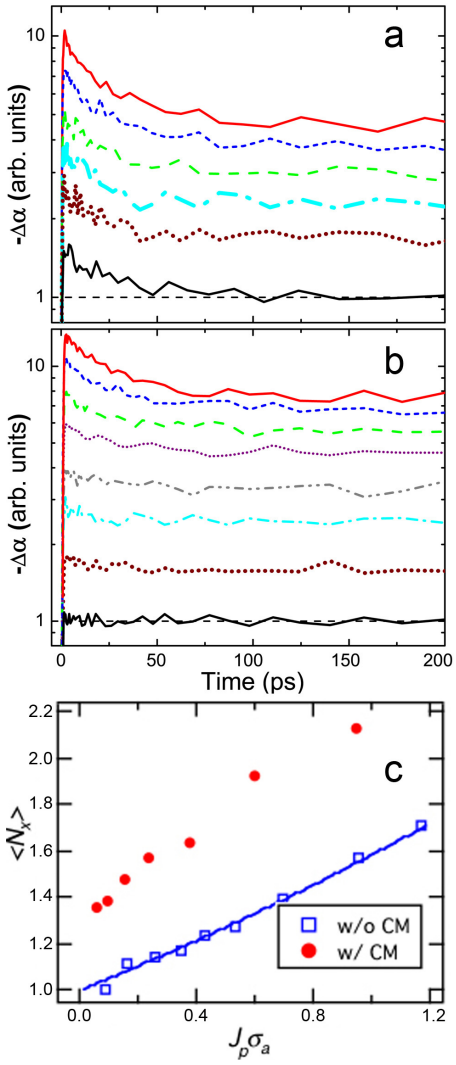

FIG. 1 (color online). 1*S* TA dynamics measured for PbSe NCs ($E_g = 0.64$ eV) as a function of excitation level using pump-photon energies $2.5E_g$ (a) (no CM) and $3.2E_g$ (b) (CM is present). The pump intensity decreases from the upper to the lower trace; $j_p\sigma_a$ changes from 1.2 to 0.09 in (a) and from 1.5 to 0.06 in (b). (c) The average exciton multiplicity as a function of pump intensity with (circles) and without (squares) CM measured using the same pump-photon energies as in (a) and (b). The data obtained for the no-CM case are well described by the dependence expected for the Poissonian distribution of carrier populations $\langle N_x\rangle = \langle N_0\rangle(1 - e^{-\langle N_0\rangle})^{-1}$, which is shown by a line.

To analyze the multiexciton ensemble produced by CM, we introduce probabilities $p_i(\hbar\omega)$ for different exciton multiplicities ($i = 1, 2, \ldots, f$). The sum of these probabilities is unity,

$$\sum_{i=1}^{f} p_i(\hbar\omega) = 1, \tag{1}$$

while the average exciton multiplicity in the ensemble of photoexcited NCs is

$$\langle N_x\rangle = \sum_{i=1}^{f} i p_i(\hbar\omega). \tag{2}$$

As we discussed in Ref. [12], probabilities p_i are directly related to rates (W_i) of generating certain multiexciton states:

$$p_i(\hbar\omega) = \frac{W_i(\hbar\omega)}{\sum_{j=1}^{f} W_j(\hbar\omega)}. \tag{3}$$

The W_i spectral dependence is approximately described by the density-of-states spectrum of the corresponding i exciton. One important feature of the CM process, which is evident from Eq. (3), is that the increasing probability for generating high-order multiexcitons with increasing spectral energy leads to *decreasing* probabilities for generating lower-order multiexcitons.

In Fig. 2(a), we show average exciton multiplicities (circles) measured for PbSe NCs of 3.9 nm radius at low pump intensities ($j_p\sigma_a \ll 1$), for which the probability for absorption of multiple photons was negligibly small. These data are compared with "ideal" multiplicities, $\langle N_x\rangle = \lfloor\hbar\omega/E_g\rfloor$, derived from energy conservation (horizontal bars). The experimental data indicate fast growth of $\langle N_x\rangle$ above the CM threshold, which can be approximated by the linear dependence $\langle N_x\rangle = 1 + 1.14(x - x_{CM})$ [line in Fig. 2(a)], where $x = \hbar\omega/E_g$ and $x_{CM} = \hbar\omega_{CM}/E_g$. Because of the steep slope (> 1), the exciton multiplicity eventually approaches its maximal value allowed by energy conservation despite the fact that the CM onset is delayed compared to the ideal value of $2E_g$ [16]. Specifically, we observe $\langle N_x\rangle = 6.9$ at $\hbar\omega = 7.8E_g$, while the ideal multiplicity is 7. The latter result indicates that CM can produce an *ensemble* state of a nearly *pure* single multiplicity.

To derive the spectral dependence of probabilities p_i we first consider the range of energies immediately above the CM threshold ($2.85E_g < \hbar\omega < 3E_g$), in which exciton multiplicity cannot exceed 2. Based on the linear growth of measured $\langle N_x\rangle$ and using Eqs. (1) and (2), we find that p_1 and p_2 are linear functions of $\hbar\omega$:

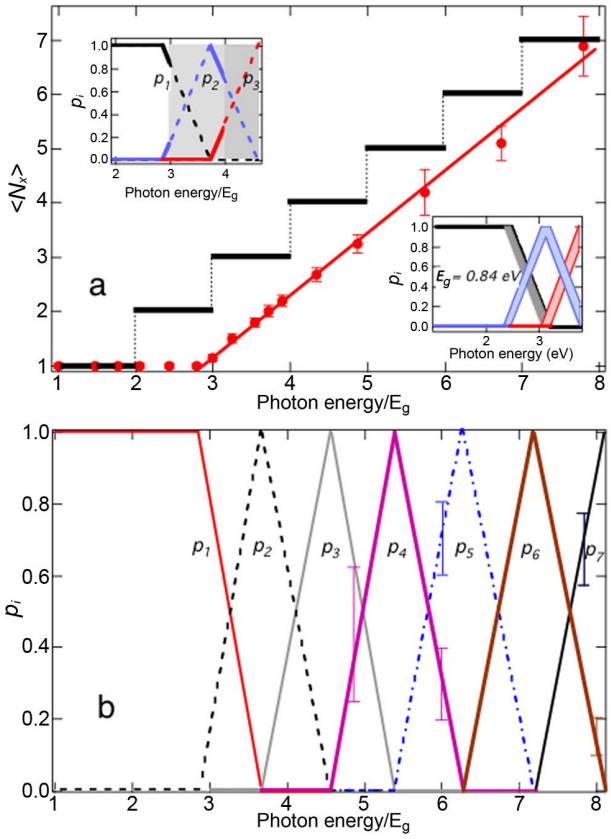

FIG. 2 (color online). (a) Measured average exciton multiplicity, $\langle N_x \rangle$, in a sample of PbSe NCs as a function of pump-photon energy normalized by E_g (circles) fit to the linear dependence with a slope $1.14/E_g$ (line). Horizontal bars forming a staircase denote ideal exciton multiplicities derived from energy conservation. Inset in the upper corner shows spectral distribution of probabilities p_1, p_2, and p_3 derived from the measured multiplicities (different style of lines corresponds to different spectral regions discussed in the text); areas with different shadings correspond to regions of different ideal multiplicities (2 and 3). Inset in the lower corner illustrates spreading of probabilities resulting from the 5% dispersion of energy gaps (the mean value of E_g is 0.84 eV). (b) Spectral distributions of probabilities p_i derived from the analysis of experimentally measured average multiplicities and carrier population dynamics. Vertical bars denote the uncertainty in a given probability derived from Eqs. (1) and (2) based only on measured $\langle N_x \rangle$ and assuming the existence of three different multiplicities.

$$p_1 = 1 - 1.14u, \qquad p_2 = 1 + 1.14u, \tag{4}$$

where $u = x - x_{\mathrm{CM}}$. For photon energies $>3E_g$, the NC ensemble can in principle also contain triexcitons. However, analysis of the measured dynamics does *not* indicate the presence of a measurable Auger-recombination triexciton component up to $3.7E_g$, i.e., up to the spectral energy for which $\langle N_x \rangle = 2$. This consideration implies that Eq. (4) is approximately valid throughout the whole range of 2.9 to $3.7E_g$ [inset in the upper corner of Fig. 2(a)], which further suggests that in this range of energies only two exciton multiplicities (1 and 2) are present in the NC ensemble; and the fraction of biexcitons can be tuned from 0 to 1 by changing $\hbar\omega$.

Another consequence of Eq. (4) is that p_1 becomes zero for $\hbar\omega \geq 3.7E_g$; it also stays zero for larger $\hbar\omega$, because of the increasing probability of generating higher-order multiexcitons, which according to Eq. (3) suppresses p_1. Using $p_1 = 0$ and taking into account that four-exciton states cannot be generated for $\hbar\omega < 4E_g$, (i.e., $p_4 = 0$), we obtain the following spectral dependence for p_2 and p_3 in the range 3.7 to $4E_g$:

$$p_2 = 2 - 1.14u, \qquad p_3 = 1.14u - 1. \tag{5}$$

Equation (4) indicates that the initial growth of p_2 that occurs above the CM threshold changes to a decrease for energies above $3.7E_g$. In the range $\hbar\omega > 4E_g$, energy conservation allows for generation of four excitons. The possibility of this additional multiplicity can only produce a faster decrease in p_2 [by increasing denominator in Eq. (3)] compared to that predicted by Eq. (5). Therefore, in this range of energies, Eq. (5) can only overestimate p_2 and hence overestimate the energy above which p_2 becomes zero. Therefore, we conclude that above $4.6E_g$ [derived from Eq. (5)], p_2 is zero, and hence at energies between 4.6 and $5E_g$, the NC ensemble can only contain two multiplicities, 3 and 4, as described by the following probabilities: $p_3 = 3 - 1.14u$ and $p_4 = 1.14u - 2$. The latter expression implies that $p_4 = 0$ for $\hbar\omega < 4.6E_g$, indicating that the range of validity of Eq. (5) extends from 3.7 to $4.6E_g$ [inset in the upper corner of Fig. 2(a)].

Using similar considerations, we can calculate probabilities up to p_7 as shown in Fig. 2(b). These probabilities have a remarkable shape of symmetric triangles, indicating a linear rise of p_i above a certain energy threshold, followed by a mirror-symmetric drop immediately after the probability reaches unity. These spectral dependences indicate that at a given photon energy only two different multiplicities are present in the NC ensemble and that there are certain energies ($x_i \approx 2 + 0.9i$; $i = 2, 3, \ldots, 7$) that produce a pure single multiplicity ensemble state.

The spectral distribution of probabilities in Fig. 2(b) is an idealized dependence that can be distorted by several factors. One such factor is the accuracy of TA measurements, which determines, e.g., the precision of a linear fit used to approximate measured average multiplicities. A possible consequence of the limited experimental accuracy is that we may miss weak contributions ($<5\%$–10% of the signal amplitude) from nondominant multiplicities in our analysis of TA data. However, even in this case, the general spectral trends predicated by Fig. 2(b) will be preserved. For example, if we assume the presence of a third multiplicity it will result in relatively small uncertainties in the p_i values shown in Fig. 2(b) by vertical bars.

Another factor that can distort the purity of an ensemble multiexciton state is dispersion of NC sizes, which leads to dispersion of energy gaps and hence a "spreading" of the spectral dependence of p_i along the $\hbar\omega$ axis [Fig. 2(a),

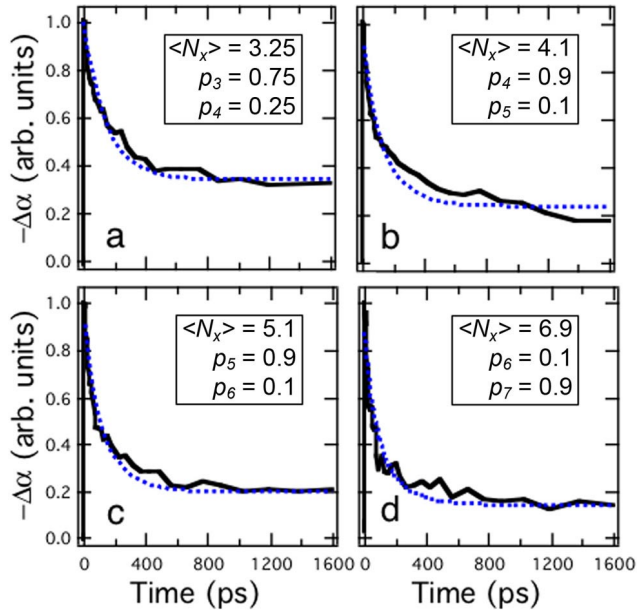

FIG. 3 (color online). $1S$ TA dynamics (solid lines) measured using photon energies $4.9E_g$ ($\langle N_x \rangle = 3.25$) (a), $5.7E_g$ ($\langle N_x \rangle = 4.1$) (b), $6.7E_g$ ($\langle N_x \rangle = 5.1$) (c), and $7.8E_g$ ($\langle N_x \rangle = 6.9$) (d); $E_g = 0.64$ eV. These dynamics are fit with no adjustable parameters (except for signal amplitude) to solutions of Eq. (6) (dotted lines) assuming that at $t = 0$ only two exciton multiplicities (with probabilities indicated in the figure) are present in the NC ensemble. The close match between experiment and modeling indicates that CM indeed produces an ensemble state that is dominated by one or two well-defined multiplicities with probabilities that can be approximately described by Fig. 2(b).

inset in the lower corner]. This effect increases the number of multiplicities that are produced in the NC ensemble for a given wavelength; it also eliminates the points of pure single multiplicities in the p_i spectra. However, even in the case of polydispersities existing in real NC samples, it is still possible to obtain an ensemble state that is dominated by one or two well-defined multiplicities as illustrated below.

In Fig. 3, we show TA dynamics measured at several spectral energies for which $\langle N_x \rangle$ varies from 3.25 to 6.9. To model these dynamics, we assume that immediately after photoexcitation ($t = 0$) only two multiplicities are present in the NC ensemble [as described by Fig. 2(b)], while the evolution of probabilities p_i in time is governed by Auger recombination [7]. In this case, p_i and p_{i-1} are coupled by the following rate equation:

$$\frac{dp_{i-1}}{dt} = \frac{p_i}{\tau_i} - \frac{p_{i-1}}{\tau_{i-1}}, \tag{6}$$

where τ_i and τ_{i-1} are the Auger-decay constants of the i and $(i-1)$ exciton states and i varies from 1 to $\lceil \langle N_x \rangle \rceil$. In our modeling, we use τ_2 values that are independently measured at high pump intensities when biexcitons are created via sequential absorption of two low-energy photons, while the decay constants of higher-order multiexcitons are calculated from the relationship $\tau_i = (2/i)^2 \tau_2$ [7]. For each excitation energy we solve Eq. (6) using Eqs. (1) and (2) and measured values of $\langle N_x \rangle$ to derive the probabilities of the two initial multiplicities ($\lfloor \langle N_x \rangle \rfloor$ and $\lceil \langle N_x \rangle \rceil$) at $t = 0$. We observe a remarkable correspondence between the calculated curves (dotted lines) and the measured dynamics (solid lines) *without* using any adjustable parameters, which indicates that the spectral dependences of p_i in Fig. 2(b) describe very closely a multiexciton ensemble in real NC samples.

In conclusion, we demonstrate that using high-efficiency CM in NCs we can produce well-defined multiexciton states with multiplicities that are highly uniform across a macroscopic NC sample. Based on the analysis of measured average exciton multiplicities, we conclude that either one or two dominant multiplicities are present in the sample at any excitation wavelength. The control over exciton multiplicity demonstrated in this work can be very useful in both fundamental studies of exciton-exciton interactions in strongly confined systems and applications that rely on multiexcitons such as lasing, nonlinear-optical switching, and quantum information processing.

This work was supported by the Chemical Sciences, Biosciences, and Geosciences Division of the Office of Basic Energy Sciences, U.S. Department of Energy, and Los Alamos LDRD funds.

*Electronic address: klimov@lanl.gov

[1] A. P. Alivisatos, Science **271**, 933 (1996).
[2] Al. L. Efros and A. L. Efros, Sov. Phys. Semicond. **16**, 772 (1982).
[3] C. B. Murray, D. J. Norris, and M. G. Bawendi, J. Am. Chem. Soc. **115**, 8706 (1993).
[4] K. I. Kang *et al.*, Phys. Rev. B **48**, 15 449 (1993).
[5] M. Achermann, J. A. Hollingsworth, and V. I. Klimov, Phys. Rev. B **68**, 245302 (2003).
[6] D. I. Chepic *et al.*, J. Lumin. **47**, 113 (1990).
[7] V. I. Klimov *et al.*, Science **287**, 1011 (2000).
[8] V. I. Klimov, J. Phys. Chem. B **104**, 6112 (2000).
[9] V. I. Klimov *et al.*, Science **290**, 314 (2000).
[10] R. D. Schaller and V. I. Klimov, Phys. Rev. Lett. **92**, 186601 (2004).
[11] R. Ellingson *et al.*, Nano Lett. **5**, 865 (2005).
[12] R. D. Schaller, V. M. Agranovich, and V. I. Klimov, Nature Phys. **1**, 189 (2005).
[13] J. M. Pietryga *et al.*, J. Am. Chem. Soc. **126**, 11 752 (2004).
[14] B. L. Wehrenberg, C. J. Wang, and P. Guyot-Sionnest, J. Phys. Chem. B **106**, 10 634 (2002).
[15] H. Du *et al.*, Nano Lett. **2**, 1321 (2002).
[16] The fact that the observed increase of $\langle N_x \rangle$ with increasing $\hbar\omega$ is faster than 1 per E_g is likely due to strong exciton-exciton interactions. Because of these interactions, the energy required to produce the N-exciton state is smaller than the ''noninteracting'' value of NE_g.